PHILLIPS

f the osphradium of *Bullia digitalis* Ste

latero-frontal cirri. *Proc. R. Soc. (B)*,
ce of the predatory starfish *Pisaster*
a (Notoacmea) scutum. Ph.D. Thesis

of the distance chemoreceptors that
tcmaea scutum (Gastropoda, Prosobra

f sensory tentacles on the mantle marg
–271.
ed ultrastrutturali sui tentacoli di
h. mikrosk. Anat., **87**, 350–376.
ultrastructure and evolutionary sig
ger, **21**, 10–18.
rvation der Kopfänhange der prosob

ution and phylogeny. *Z. Zool. Syst.*

rosobranchen Schnecken *Buccinum*
95, 317–330.
ne slug, *Arion ater* (Pulmonata, Mo
thelium. *Cell. Tiss. Res.*, **151**, 245–25
nd function of scolopophorous sensil
, **56**, 246–259.
Ultrastructural studies on the epithe
oidea). *Cell Tiss. Res.*, **172**, 245–26
l sensory cells in the freshwater snails
, **22**, 283–298.

Petit

& CELL 1979 **11** (4) 633–642
ed by Longman Group Ltd. Printed in Great Britain

HENRI PETIT, WALTER L. DAVIS and RUTH JONES

MORPHOLOGICAL STUDIES ON THE PERIOSTRACUM OF THE FRESH-WATER MUSSEL *AMBLEMA* (UNIONDAE): LIGHT MICROSCOPY, TRANSMISSION ELECTRON MICROSCOPY, AND SCANNING ELECTRON MICROSCOPY

ABSTRACT. The structure of the periostracum in the fresh-water mussel *Amblema* has been described using light microscopy, transmission electron microscopy, and scanning electron microscopy. The structure and evolutive course of the periostracum was studied along its entire length, from the periostracal groove until it forms the tough outer covering of the shell. At least five structurally and functionally distinct regions were identified. In addition, the periostracum itself was seen to be a multilayered structure consisting of three major layers which are themselves subdivided into minor layers. From these morphological observations, a regulatory role for the various periostracal layers in mineral trapping, nucleation, and the subsequent formation of the prismatic and nacreous layers of the shell can be postulated.

Introduction

The periostracum has been considered obviously as simply the outer waterproof covering of the shell. Thus, it represents the outer layer of most molluscan shells. Its structure and chemical composition were first described by Haas (1935) and later confirmed and elaborated on by numerous other investigators (Beedham, 1958; Beedham and Trueman, 1965; Wada, 1966; Wilbur and Saleuddin, 1968; Meenakshi *et al.*, 1969; Taylor and Kennedy, 1969).

Most studies agree that the periostracum is elaborated by the epithelial cells of the inner surface of the outer mantle fold (Korringa, 1951; Brown, 1952; Yonge 1957; Beedham, 1958; Hillman, 1961). The ultrastructural morphology of the cells and the cellular mechanisms involved in this process have been described (Bevelander and Nakahara, 1967, 1970; Wada, 1968; Saleuddin, 1974, 1975).

From the above literature survey, as well as a gross morphological evaluation of the periostracum, its structure appeared to be that of a simple uniform entity. However, from our observations reported here, this mantle product demonstrates a complex multilayered organization and is dramatically different, both morphologically and functionally, along its entire course. Some previous investigators have advocated that the periostracum, its inner part, serves as a nucleation site for the precipitation and growth of calcium carbonate crystals (Taylor and Kennedy, 1969; Nakahara and Bevelander, 1971). We generally agree with these authors, but believe that the mechanism, that is the total functional role of the periostracum in shell formation, has remained virtually incomplete and poorly understood. To better understand the physiology of the periostracum, one must comprehend its structure, along its entire course, from its

Department of Microscopic Anatomy, Baylor College of Dentistry Dallas, Texas.

Received 15 May 1979.

point of origin in the periostracal groove until it becomes the outer covering of the mineralized shell. Using various microscopic techniques, we report here the functional morphology of the periostracum in the freshwater mussel *Amblema*.

Materials and Methods

Specimens of *Amblema plicata perplicata* Conrad, a fresh-water Uniondae, were obtained from a local lake. Animals were maintained in the laboratory in environmentally regulated stock aquaria.

For sacrifice, animals were placed overnight in a 4°C refrigerator. This produced a slight opening of the valves (Petit *et al.*, 1978). With a diamond saw (Cab Mate, Graves Co., Del Ray Beach, Fla.), irrigated with fixative, either phosphate buffered formalin (Carson *et al.*, 1973) or 2·5% glutaraldehyde buffered with 0·1 M cacodylate (pH 7·4), small regions of the shell with its attached periostracum and mantle edge were removed in their relative *in vivo* relationships. These sections were subsequently placed in their appropriate fixative.

Following post-osmication in either phosphate or cacodylate buffered (pH 7·4) 1% osmium tetroxide, some tissues were prepared for scanning electron microscopy by acetone dehydration and subsequent critical point-CO_2 drying (Anderson, 1951). Other tissues were alcohol dehydrated, flat embedded (to insure proper orientation) in low viscosity medium (Spurr, 1969) and eventually sectioned for light microscopic and transmission electron microscopic observation. For light microscopy, 1·0–2·0 μm sections were stained with paragon (Martin *et al.*, 1967). Thin sections for transmission electron microscopy, showing gold–silver interference colors, were mounted on uncoated copper grids and subsequently double stained with uranyl acetate and lead citrate (Reynolds, 1963).

To demonstrate inorganic ions, primarily calcium, sections of mantle edge were manually dissected and placed immediately in osmium-pyroantimonate (Carson *et al.*, 1978; Davis *et al.*, 1979). Following a 2–4 hr

Fig. 1. Light micrograph demonstrating the extrusion of the periostracal ribbon (pellicle) from the periostracal groove. The ribbon is closely adhered to the low cuboidal epithelial cells of the periostracal groove (arrowheads). Glutaraldehyde fixation, Paragon stain. ×400.

Fig. 2. Transmission electron micrograph (TEM) of periostracum formation. Note that the microvilli appear to be adhered to the forming periostracum. This may result in direct glycocalyx (arrows) deposition (proteinaceous deposition) onto the pellicle surface. Glutaraldehyde fixation. ×20,000.

Fig. 3. TEM of periostracum formation. Note that the periostracum shows no contact with the epithelial cells. Also note the proteinaceous glycocalyx material on either side (inner, i; outer o) of the pellicle. Thus, both epithelial cell layers lining the periostracal groove may secrete material which is adsorbed to the surface of the forming pellicle. This material is pyroantimonate positive, especially along the columnar cells (Co). Osmium-pyroantimonate fixation. Cu, cuboidal cells. ×11,300.

Fig. 4. Scanning electron micrograph (SEM) of the periostracum within the periostracal groove. Amorphous mineral granules (arrowheads) are seen on the inner surface of the pellicle. These are apparently trapped and conveyed toward the shell edge by the forming periostracum. Glutaraldehyde fixation. ×1000.

Fig. 5. Light micrograph demonstrating the extensive foliation of the inner layer of the periostracum (arrows). Glutaraldehyde fixation. C, periostracal *cul de sac*. ×100.

Fig. 6. TEM of the periostracal foliations shown in Fig. 5. Note the accumulation of pyroantimonate positive material (arrowheads) in this pouch-like structure. Osmium-pyroantimonate fixation. C, periostracal *cul de sac*. ×12,800.

subsequently placed in their
fixative.

owing post-osmication in either
or cacodylate buffered (pH
n tetroxide, some tissues
for scanning electron micro
e dehydration and subsequent
CO_2 drying (Anderson, 1951)
were alcohol dehydrated,
(to insure proper orientation)
y medium (Spurr, 1969) and
ctioned for light microscop
ssion electron microscopic
for light microscopy,
were stained with paragon (M
967). Thin sections for transmis
microscopy, showing gold
nce colors, were mounted on
copper grids and subsequ
tained with uranyl acetate and
Reynolds, 1963).

monstrate inorganic ions, primar
sections of mantle edge were
ected and placed immediately
pyroantimonate (Carson *et*
vis *et al.*, 1979). Following a

he extrusion of the periostracal
ribbon is closely adhered to the
groove (arrowheads). Glutaraldeh

TEM) of periostracum formation.
forming periostracum. This may
einaceous deposition) onto the pellicle

Note that the periostracum shows
proteinaceous glycocalyx material
us, both epithelial cell layers lining the
s adsorbed to the surface of the forming
ve, especially along the columnar
boidal cells. × 11,300.

of the periostracum within the per
owheads) are seen on the inner surface
conveyed toward the shell edge by the
× 1000.

xtensive foliation of the inner layer
ion. C, periostracal *cul de sac*.

n in Fig. 5. Note the accumulation
n this pouch-like structure. Osmium
ac. × 12,800.

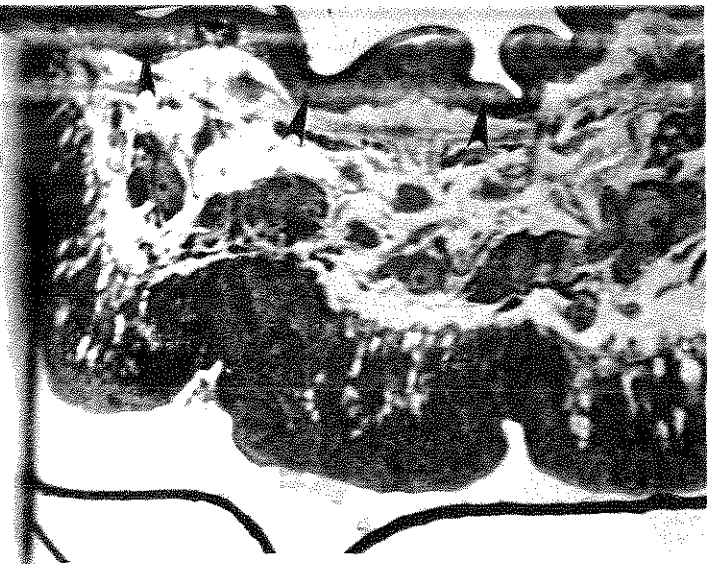

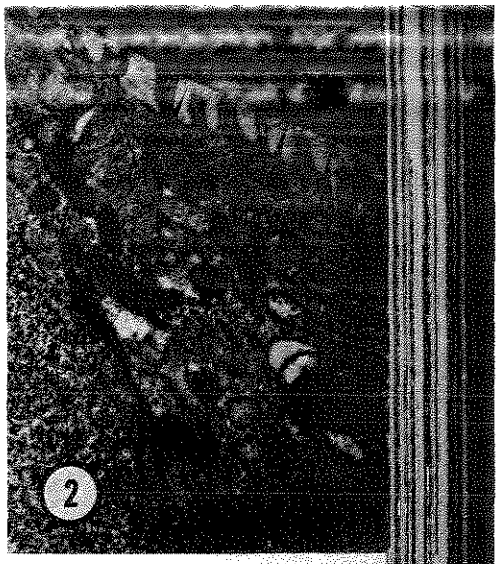

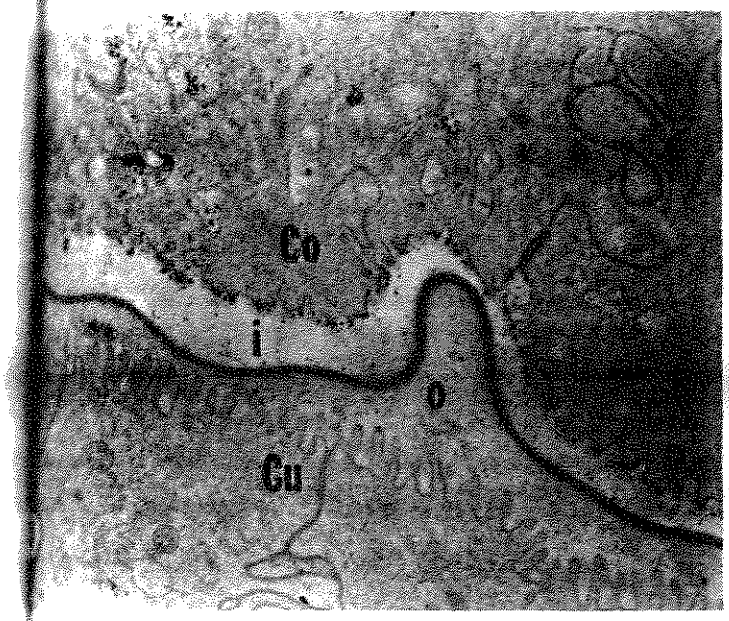

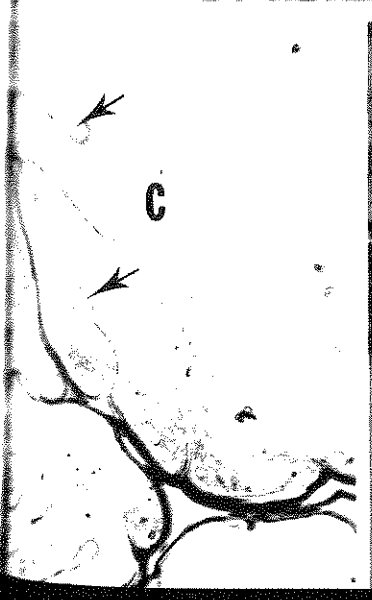

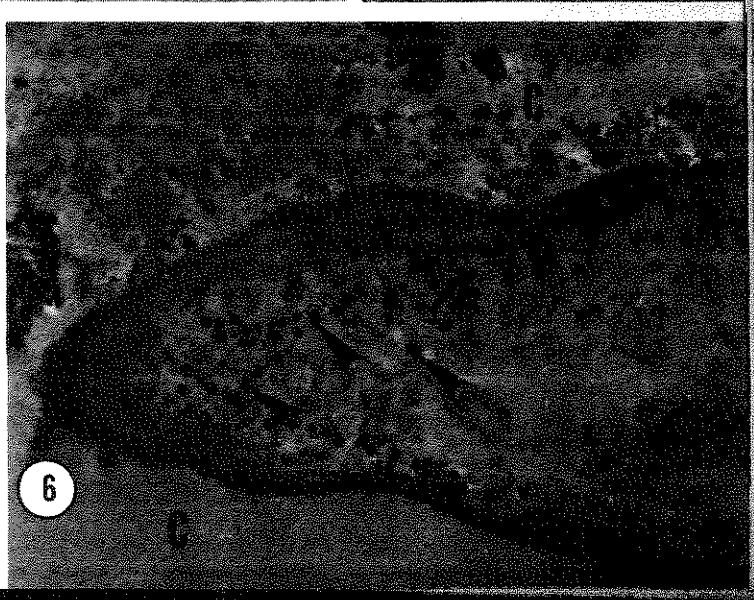

fixation period, tissues were washed several times in deionized water, dehydrated in ethanol and embedded in Spurr medium as above. Thin sections were prepared as indicated previously.

Dried tissues were coated with gold-palladium and examined in an AMR 1000 scanning electron microscope (Advanced Metals Research Corp., Burlington, Mass.) operated at 20 kV. Thin sections were viewed in a Philips 300 transmission electron microscope (Philips Electronic Instruments, Inc., Mt Vernon, N.Y.) operated at 40–100 kV.

Results

Periostracum inside the periostracal groove

The formation and course of the periostracum within its groove is demonstrated in Fig. 1. The pellicle is formed on the epithelial cells lining the inner surface of the outer ridge of the periostracal groove. Fig. 2 is a transmission electron micrograph of the proteinaceous deposition on to the pellicle surface. In some instances, microvilli of epithelial cells are directly adhered to the forming pellicle (Fig. 2). In other instances (Fig. 3), the pellicle is without direct contact by the adjacent epithelial cells. In Fig. 3, it appears as if a homogeneous material, apparently secreted by cells lining the periostracal groove, is coating both surfaces of the forming periostracum. Some pyroantimonate positive granules (calcium?) are seen within this fluid layer, and on the surface of epithelial microvilli. These are especially prevalent on the inner surface of the evolving periostracum.

Fig. 4 is a scanning electron micrograph of the inner surface of the periostracum within the periostracal groove. It demonstrates amorphous mineral granules (deposits) which are probably adhered to and conveyed toward the shell edge by the forming periostracum.

The periostracal reflection forming the cul de sac (foliation and nacreous deposition)

In this portion of the periostracum, an extensive foliation of the inner periostracal layer occurs (Fig. 5). This forms highly folded curtains which penetrate deeply into the *cul de sac* fluid (Fig. 5). Such folds probably serve to trap and precipitate mineral ions as demonstrated by pyroantimonate electron microscopy (Fig. 6). After a

Fig. 7. TEM of fibrillar extensions of the inner periostracum. After the layers of the periostracum re-unite, proteinaceous extensions (arrows) of the inner periostracum appear to initiate and regulate the subsequent mineralization phenomenon. Glutaraldehyde fixation. × 14,000.

Fig. 8. TEM of the initial formation and mineralization of the nacreous layer. The crystallized nacreous laminae appear to be bordered by the proteinaceous fibrils (arrows) initially described in Fig. 7. Glutaraldehyde fixation. × 6100.

Fig. 9. TEM of the periostracum demonstrating vacuole formation (V) in the middle layer of the periostracum. Note the presence of pyroantimonate reaction product within the vacuoles (arrow). Osmium-pyroantimonate fixation. × 4000.

Fig. 10. SEM through the middle periostracal layer demonstrating the spherical crystalline subunits (arrowheads). These initially form in the vacuoles described in Fig. 9 and subsequently give rise to the prismatic layer of the shell. Glutaraldehyde fixation. × 1100.

Fig. 11. Light micrograph of the cleaving periostracum. The inner aspect (arrow) cleaves to cover the outer nacre, while the outer portion (arrowhead) covers the outermost portion of the shell. Proteinaceous fibrils (small arrowheads) extend between the cleaving layers. Glutaraldehyde fixation. × 100.

Fig. 12. SEM of vacuole formation (arrows) in the periostracum. These eventually fuse and produce the separation of the periostracum layers described in Fig. 11. Glutaraldehyde fixation. × 5000.

epithelial cells. In Fig. 3, a homogeneous material, ed by cells lining the perio coating both surfaces of the cum. Some pyroantimonate (calcium?) are seen within and on the surface of illi. These are especially nner surface of the evolving

ning electron micrograph of of the periostracum within groove. It demonstrates al granules (deposits) which dhered to and conveyed edge by the forming perio

eflection forming the cul de nacreous deposition)

of the periostracum, an of the inner periostracal g. 5). This forms highly hich penetrate deeply into luid (Fig. 5). Such folds to trap and precipitate demonstrated by pyroanti- nicroscopy (Fig. 6). After a

stracum. After the layers of the ws) of the inner periostracum ation phenomenon. Glutaralde-

ion of the nacreous layer. The by the proteinaceous fibrils xation. ×6100.

ole formation (V) in the middle oantimonate reaction product ixation. ×4000.

r demonstrating the spherical in the vacuoles described in r of the shell. Glutaraldehyde

um. The inner aspect (arrow (arrowhead) covers the outer- rowheads) extend between the

periostracum. These eventually layers described in Fig. 11

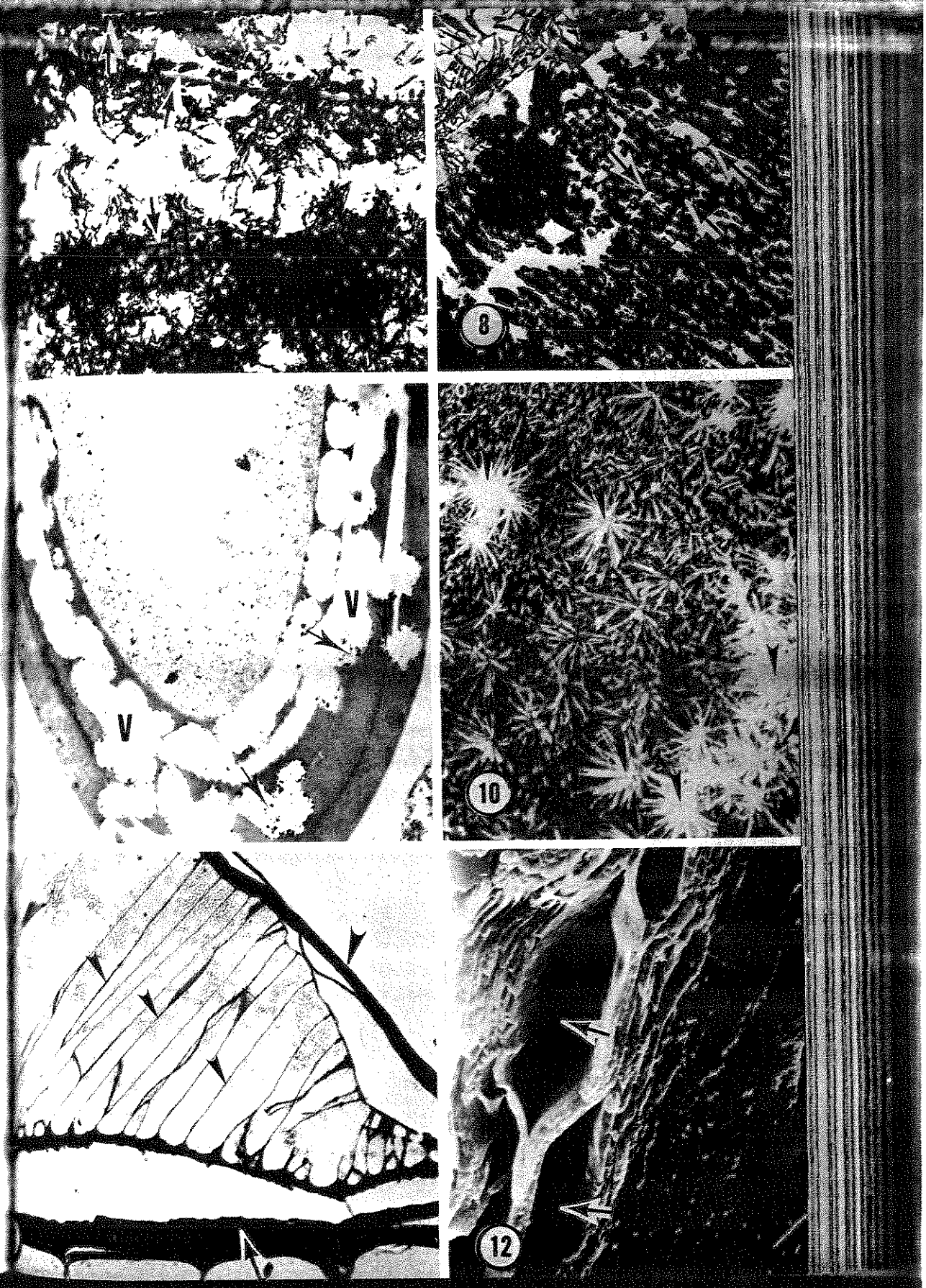

while, the multiple layers of the periostracum again meet and fuse while, simultaneously, the mineral is organized on the inner surface of the periostracum. This mineral organization is apparently governed by parallel fibrils (laminae) of proteinaceous extensions originating from the inner periostracal layer (Fig. 7). Such organic material may serve as a primary template for the initial mineral seeding and subsequent subunit formation, packing, and stacking (Fig. 8), characteristic of the nacreous layer.

At the same time, structural changes are occurring in the other layers of the periostracum. The middle periostracal layer becomes highly vacuolated (Fig. 9). These new compartments serve to collect the mineral and subsequently organize it into spherical crystalline balls (Fig. 10), which are the elementary subunits of the prismatic layer (see below).

Prismatic differentiation of the periostracum

Here, the freedom of the periostracum is limited by its attachment to the already formed edge. At this point, the layers of the periostracum cleave to cover the outermost part of the shell and the outermost layer of the nacre (Fig. 11). This separation begins as ovoid vacuoles (Fig. 12) which eventually fuse and stretch to become columns of organic matrix extending between the diverging periostracal layers (Figs. 11, 13). The mineral is first arranged in spherical subunits within these vacuoles. These are subsequently packed within the columns to form the prisms. Some elementary needles persist; these are driven toward the forming side of the prism. Some columns divide and form the interprismatic bags. Inside the huge chambers formed by vacuolar fusion, mineral is driven and organized into spherical subunits. The honeycomb-like pattern of the prismatic matrices (as seen in transverse section) is shown on the periostracum before the new calcification (reorganization) front is formed (Fig. 14). Fig. 15 demonstrates the subunit packing within the chambers. Further details on the formation of the prismatic layer will be described in a later publication.

Attached periostracum

Fig. 16 shows the crude edge on which the periostracum is attached. Note that the partitions between the prisms are not the columns we have previously described (Fig. 13). On a partially decalcified preparation (Fig. 17), the matrices appear to be a further condensation of the original proteinaceous matrices (columns) and are morphologically the result of the secondary crystallization into the prismatic units.

The outer layer of the periostracum is difficult to morphologically differentiate

Fig. 13. SEM of the early stages of cleavage of the periostracum. Vacuoles, walled by organic matrices (arrows), are clearly evident. Glutaraldehyde fixation. × 2000.

Fig. 14. SEM demonstrating the honeycomb-like arrangement of the periostracum prior to calcification of the prismatic layer. Osmium fixation. × 500.

Fig. 15. SEM demonstrating subunit loading or packing of the matricial chambers of the future prismatic layer. Osmium fixation. × 2000.

Fig. 16. SEM of the shell edge. The periostracum and the matrices of the prismatic layer (arrows) are seen. There are no complete prisms in this micrograph. The base or open end of the matricial prismatic bags is obliterated by nacreous deposition (N). Glutaraldehyde fixation. × 250.

Fig. 17. SEM of the prismatic matrices with contained mineralized material (arrows). Slightly decalcified by gentle treatment with HCl. Note that the walls of the prisms are not the initial columns described in Fig. 13. × 800.

Fig. 18. SEM of the inner aspect of the periostracum as it covers the shell. Note the presence of pores. Prismatic matrices are also seen (arrow). Glutaraldehyde fixation. × 2000.

T. DAVIS AND JONES

Figs. 11, 13). The mineral
spherical subunits within
e are subsequently packed
to form the prisms. Some
persist; these are driven
side of the prism. Some
form the interprismatic
ge chambers formed by
neral is driven and organ
ubunits. The honeycomb
prismatic matrices (as
ection) is shown on the
e the new calcification
nt is formed (Fig. 14).
tes the subunit packing
s. Further details on the
prismatic layer will be
publication.

um

rude edge on which the
ttached. Note that the
the prisms are not the
reviously described (Fig.
decalcified preparation
es appear to be a further
e original proteinaceous
and are morphologically
secondary crystallization
nits.
of the periostracum is
hologically differentiate

stracum. Vacuoles, walled by
hyde fixation. ×2000.

ngement of the periostracum
tion. ×500.

of the matricial chambers of

the matrices of the prismatic
this micrograph. The base of
by nacreous deposition (N).

mineralized material (arrows)
at the walls of the prisms are

it covers the shell. Note the
w). Glutaraldehyde fixation.

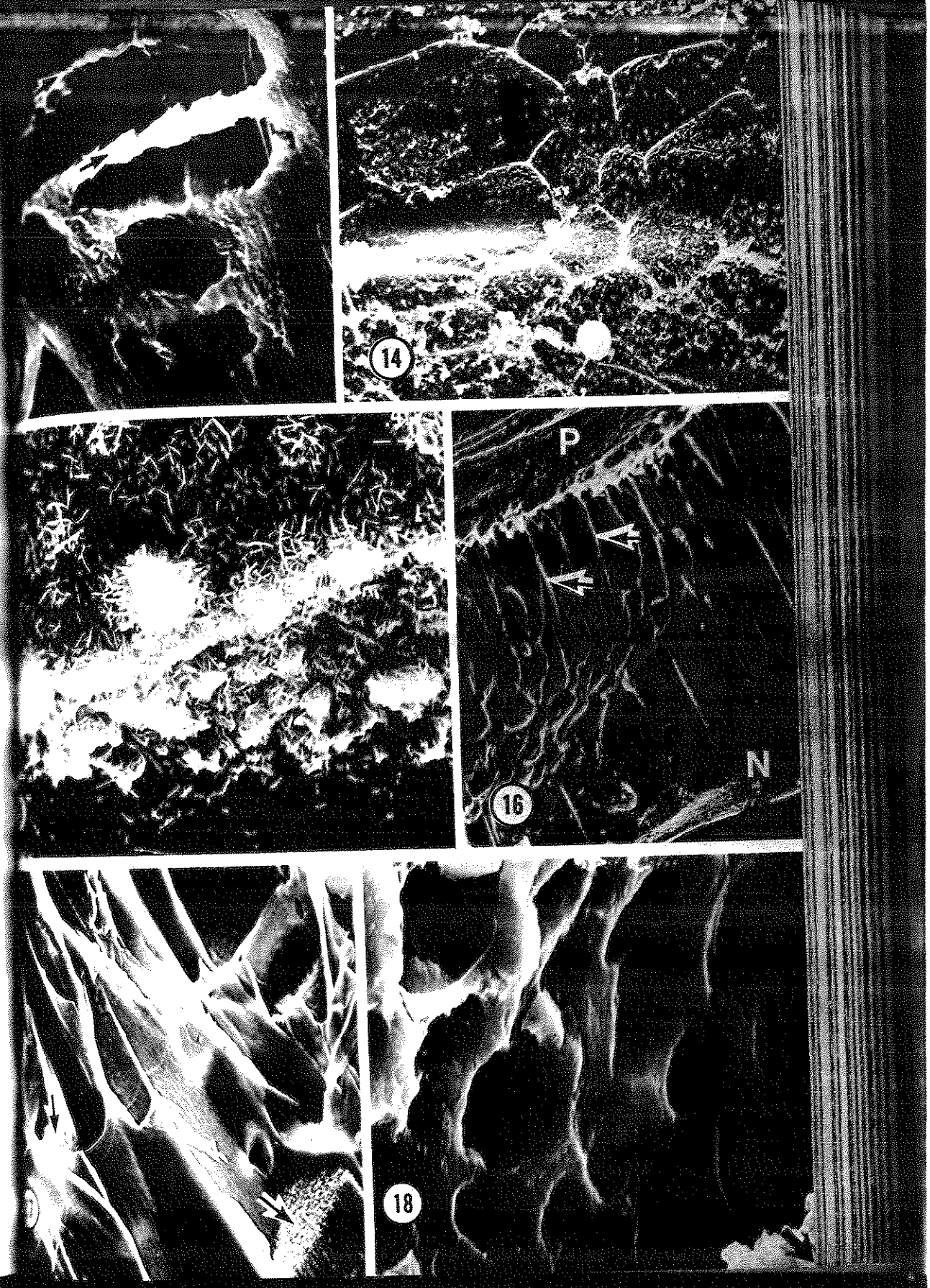

from the matricial prism bags, but can be easily peeled (reflected) from the top of the prismatic matricial bags. In this case, it appears as porous a structure on its inner surface (Fig. 18). Pores were also seen on the outer surface as well.

Discussion

Fig. 19 is a diagrammatic representation of the morphology, the various regions of, and the evolutive course of the periostracum in the fresh-water mussel *Amblema*. At least five distinct regions of this structure are clearly demarcated. These are: (1) the forming pellicle inside the periostracal groove; (2) the foliated part, characterized by extensive infoldings of the inner layer of the periostracum; (3) laminar extensions indicative of nacreous differentiation; (4) vacuole formation indicative of prismatic differentiation; (5) and when the periostracum becomes the tough outer covering of the mineralized shell. The structure of the periostracum is markedly different in each of the above areas; however, the transition between the respective zones appeared to be smooth rather than abrupt.

Previous ultrastructural observations by other investigators have examined only the initial steps in the formation of the periostracum in either the periostracal groove or gland (Bevelander and Nakahara, 1967, 1970; Saleuddin, 1974, 1975). To our knowledge, no fine structural investigations have reported both the structure and evolutive

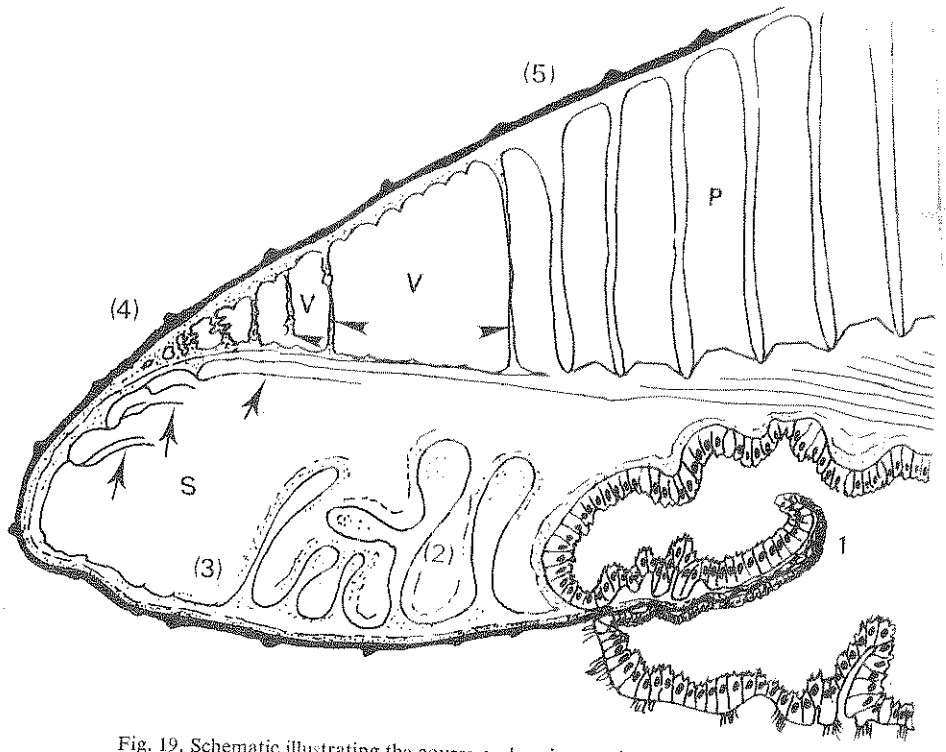

Fig. 19. Schematic illustrating the course and various regions of the periostracum in *Amblema*. The circled numbers (1–5) indicate the five described regions of the periostracum: (1) in the periostracal groove; (2) where the inner layer of the periostracum becomes extensively foliated; (3) after the layers rejoin, the periostracum is reflected and its inner layer produces proteinaceous laminae (arrows) which function in the formation of the nacre (N); (4) following the bifurcation of the periostracum vacuole formation (V) and the resultant production of colums of organic matrix (arrowheads) function in the formation of the prismatic layer (P); (5) where the periostracum becomes attached to the shell as its outermost layer. S, periostracal *cul de sac*.

m; (3) laminar extensions indi-
creous differentiation; (4) vacuole
ndicative of prismatic differenti-
and when the periostracum be-
ugh outer covering of the mineral-
he structure of the periostracum
different in each of the above
ever, the transition between the
zones appeared to be smooth
abrupt.

ultrastructural observations by
igators have examined only the
in the formation of the perio-
either the periostracal groove or
elander and Nakahara, 1967;
ddin, 1974, 1975). To our know-
ne structural investigations have
th the structure and evolution

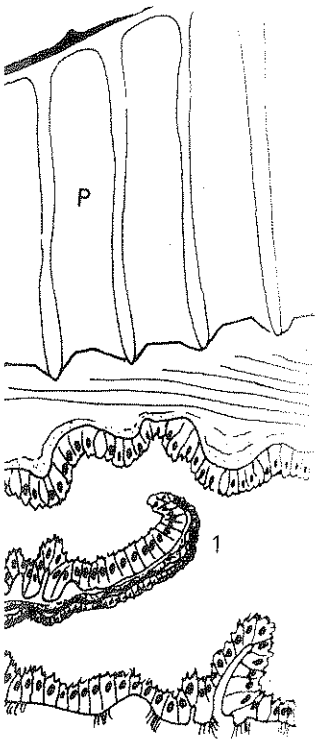

ns of the periostracum in
bed regions of the perio-
layer of the periostracum
periostracum is reflected
s) which function in the
he periostracum, vacuole
anic matrix (arrowheads)
where the periostracum
stracal *cul de sac*.

course of the periostracum along its entire
ree and attached lengths, from the perio-
stracal groove to the outer shell surface.

We observed and confirmed the structure of
he periostracum to be multilayered, con-
sisting of at least three major layers which
themselves are further subdivided into sub-
unit layers. The multilayered nature of the
periostracum has been reported previously
(Needham, 1965; Bevelander and Nakahara,
1967). From our study described here, it
appears that the periostracal layers develop
through the accretion of proteinaceous
material on to the intial pellicle. This occurs
at the periostracal groove where apparently
the subsequent behavior and structure
(morphodifferentiation) of the periostracum is
monitored. For example, the outer layer is
hardened and forms the incremental growth
lines; the middle or vacuolated layer
receives the calcium load for the formation of
the prismatic layer; and the inner layer begins
to fold, trapping the mineral components of
the future nacre and eventually aligning these
crystals on to laminar extensions. This
elaboration occurs just as the periostracum
emerges from its groove. Thus, specific chemical
and mechanical (attached *vs.* free; vacuo-
lated *vs.* foliated) differences apparently
regulate the form and function of the perio-
stracum. In addition, the process of ion
trapping and binding, and further protein
accretion onto its primary structure, serve to
alter its macromolecular configuration and
hence its activity and function, which are
closely intricated.

As a result of our morphologic observations,
the periostracum appears to play a major
regulatory role in both nacreous and pris-
matic elaboration, formation, and orienta-
tion (crystalline) at the growing edge of the
molluscan shell and, therefore, cannot be
considered any more as being limited only to
the outer tanned waterproof covering of the
shell which is inactive and often eroded as
was consistently seen on the beak surfaces of
Amblema. Details regarding the role of the
periostracum in the formation of the pris-
matic and nacreous shell layers will be
described in a forthcoming communication
(Petit, Jones and Davis, in preparation).

Acknowledgements

The authors gratefully acknowledge the
excellent manuscript preparation and secre-
tarial assistance provided by Jane Coleman.

References

ANDERSON, T. F. 1951. Techniques for the preservation of three-dimensional structure in preparing specimens for the electron microscope. *Trans. N.Y. Acad. Sci., Sec. II*, **13**, 130–134.

BEEDHAM, G. E. 1958. Observations on the non-calcareous components of the shell of lamellibranchia. *Qt. Jl Microsc. Sci.*, **99**, 341–357.

BEEDHAM, G. E. and OWEN, G. 1965. The mantle and the shell of *Solamya parkensoni* (protobranchia: bivalvia). *Proc. Zool. Soc. Lond.*, **144**, 405–430.

BEVELANDER, G. and NAKAHARA, H. 1967. An electron microscope study of the formation of the periostracum of *Macrocallista maculata*. *Calc. Tiss. Res.*,**1**, 55–67.

BEVELANDER, G. and NAKAHARA, H. 1970. An electron microscope study of the formation and structure of the periostracum of a gastropod, *Littorina littorea*. *Calc. Tiss. Res.*, **5**, 1–12.

BLOUNT, C. H. 1952. Some structural proteins of *Mytilus edulis*. *Q. Jl. Microsc. Sci.*, **93**, 487–502.

CARSON, F. L., MARTIN, J. H. and LYNN, J. A. 1973. Formalin fixation for electron microscopy: a re-evaluation. *Am. J. clin. Pathol.*, **59**, 365–373.

CARSON, F. L., DAVIS, W. L., MATTHEWS, J. L. and MARTIN, J. H. 1978. Calcium localization in normal, rachitic and D_3-treated chicken epiphyseal chondrocytes utilizing potassium pyroantimonate-osmium tetroxide. *Anat. Rec.*, **109**, 23–40.

DAVIS, W. L., JONES, RUTH G. and HAGLER, H. K. 1979. Calcium containing lysosomes in the normal chicken duodenum: a histochemical and analytical electron microscopic study. *Tissue & Cell*, **11**, 127–138.

GRAS, F. 1935. Bivalvia, II. Die Schale. In *Bronns Klassen und Ordung des Tier-Reichs* (ed. H. G. Brown), Bd. iii, Abt. 3. Bivalvia, Tiel 1.

HOFFMAN, R. E. 1961. Formation of the periostracum in *Mercenaria mercenaris*. *Science*, **134**, 1754–1755.

KORRINGA, P. 1951. On the nature and function of chalky deposits in the shell of *Ostrea edulis* Linn. *Proc. Calif. Acad. Sci.*, **27**, 133–158.
MARTIN, J. H., LYNN, J. A. and Nickey, W. M. 1967. A rapid polychrome stain for epoxy embedded tissues. *Am. J. clin. Pathol.*, **46**, 250–251.
MEENAKSHI, V. R., HARE, P. E., WATABE, N. and WILBUR, K. M. 1969. The chemical composition of the periostracum of the molluscan shell. *Comp. Biochem. Physiol.*, **29**, 611–620.
NAKAHARA, H. and BEVELANDER, G. 1971. The formation and growth of the prismatic layer of *Pinctada radiata*. *Calc. Tiss. Res.*, **7**, 31–45.
PETIT, H., DAVIS, W. L. and JONES, RUTH, G. 1978. Morphological studies on the mantle of the fresh-water mussel *Amblema* (Unionidae): scanning electron microscopy. *Tissue & Cell*, **10**, 619–627.
REYNOLDS, E. S. 1963. The use of lead citrate at high pH as an electron-opaque stain in electron microscopy. *J. Cell Biol.*, **17**, 208–212.
SALEUDDIN, A. S. M. 1974. An electron microscopic study of the formation and structure of the periostracum in *Astarte* (bivalvia). *Can. J. Zool.*, **52**, 1463–1471.
SALEUDDIN A. S. M. 1975. An electron microscopic study on the formation of the periostracum in *Helisoma* (Mollusca). *Calc. Tiss. Res.*, **18**, 297–310.
SPURR, A. R. 1969. A low-viscosity epoxy resin embedding medium for electron microscopy. *J. Ultrastruct. Res.*, **26**, 31–43.
TAYLOR, J. D. and KENNEDY, W. J. 1969. The influence of the periostracum on the shell structure of bivalve molluscs. *Calc. Tiss. Res.*, **3**, 274–283.
WADA, K. 1966. Spiral growth of nacre. *Nature, Lond.*, **211**, 1427
WADA, K. 1968. Electron microscopic observations of the formation of the periostracum in *Pinctada fucata*. *Bull. Nat. Pearl Res. Lab.*, **13**, 1540–1560.
WILBUR, K. M. and SIMKISS, K. 1968. Calcified shells. In *Comprehensive Biochemistry* (eds. M. Florkin and E. H. Stotz), Vol. 26A, pp. 229–295. Elsevier, New York.
YONGE, C. M. 1957. Mantle fusion in the lamellibranchia. *Publ. Staz. Zool. Napoli*, **29**, 151–171.